A Hedgehog-Induced BTB Protein Modulates Hedgehog Signaling by Degrading Ci/Gli Transcription Factor

Qing Zhang,[1,4] Lei Zhang,[1,4] Bing Wang,[1]
Chan-Yen Ou,[3] Cheng-Ting Chien,[3] and Jin Jiang[1,2,*]
[1] Center for Developmental Biology
[2] Department of Pharmacology
University of Texas Southwestern Medical Center
   at Dallas
Dallas, Texas 75390
[3] Institute of Molecular Biology
Academia Sinica
Taipei
Taiwan

Summary

The Ci/Gli family of transcription factors mediates Hedgehog (Hh) signaling in many key developmental processes. Here we identify a Hh-induced MATH and BTB domain containing protein (HIB) as a negative regulator of the Hh pathway. Overexpressing HIB downregulates Ci and blocks Hh signaling, whereas inactivating HIB results in Ci accumulation and enhanced pathway activity. HIB binds the N- and C-terminal regions of Ci, both of which mediate Ci degradation. HIB forms a complex with Cul3, a scaffold for modular ubiquitin ligases, and promotes Ci ubiquitination and degradation through Cul3. Furthermore, HIB-mediated Ci degradation is stimulated by Hh and inhibited by Suppressor of Fused (Sufu). The mammalian homolog of HIB, SPOP, can functionally substitute for HIB, and Gli proteins are degraded by HIB/SPOP in Drosophila. We provide evidence that HIB prevents aberrant Hh signaling posterior to the morphogenic furrow, which is essential for normal eye development.

Introduction

The Hedgehog family of morphogens controls pattern formation and tissue homeostasis through the Ci/Gli family of transcription factors (Ingham and McMahon, 2001; Jia and Jiang, 2006). Aberrant Hh signaling that leads to uncontrolled Gli activity has been linked to many human diseases including cancer (Pasca di Magliano and Hebrok, 2003; Villavicencio et al., 2000). As such, the activity of Ci/Gli is tightly monitored through multiple levels of regulation including phosphorylation, proteolysis, nuclear-cytoplasmic partitioning, and protein-protein interactions (Jia and Jiang, 2006; Lum and Beachy, 2004). In Drosophila, the full-length Ci (Ci^{FL}) is phosphorylated by multiple kinases including protein kinase A (PKA), glycogen synthase kinase 3 (GSK3), and casein kinase I (CKI) in the absence of Hh (Jia et al., 2002, 2005; Price and Kalderon, 2002). Phosphorylation recruits the Slimb-Cul1-based E3 ubiquitin ligase that targets Ci^{FL} for ubiquitin/proteasome-mediated proteolysis to generate a truncated repressor form (Ci^{Rep}) (Jia

*Correspondence: jin.jiang@utsouthwestern.edu
[4] These authors contributed equally to this work.

et al., 2005; Smelkinson and Kalderon, 2006). Ci^{FL} also forms complexes with the kinesin-like protein Costal2 (Cos2), the Ser/Thr kinase Fused (Fu), and Sufu (Monnier et al., 1998; Robbins et al., 1997; Sisson et al., 1997), which regulate phosphorylation, nuclear translocation, and transcriptional activator activity of Ci^{FL} (Methot and Basler, 2000; Ohlmeyer and Kalderon, 1998; Wang et al., 2000).

In the Drosophila eye disc, Hh secreted from differentiating cells posterior to the morphogenic furrow (MF) induces the expression of dpp required for the anterior progression of the MF (Treisman and Heberlein, 1998). In contrast to wing or leg disc where Ci is expressed only in Hh-responding cells but not in Hh-producing cells, Ci is expressed uniformly in eye disc; however, Ci^{FL} protein level is kept low posterior to the MF by Cul3-mediated degradation (Ou et al., 2002). Although Cul3 is uniformly expressed in the eye disc, loss of Cul3 only affects Ci^{FL} posterior to the MF, implying that Cul3-based ubiquitin ligase activity is restricted posterior to the MF. Recently, it has been shown that BTB (Broad Complex, Tramtrack, and Bric a Brac) proteins function as substrate recognition subunits for Cul3-based modular ubiquitin ligases (Pintard et al., 2004). These BTB proteins contain one or more BTB domains that interact with Cul3 and other protein-protein interacting domains, including the meprin and TRAF homology (MATH) domain that bind substrates (Pintard et al., 2003; Xu et al., 2003). We hypothesized that a spatially restricted BTB protein(s) may act in conjunction with Cul3 to degrade Ci^{FL} posterior to the MF.

In this study, we identified a BTB protein named HIB that is expressed posterior to the MF in the Drosophila eye disc and is responsible for downregulating Ci in differentiating cells. We provide evidence that HIB is the substrate recognition component of a Cul3 E3 ubiquitin ligase that targets Ci for degradation. Interestingly, HIB expression is induced by Hh signaling. Hence, HIB provides a negative feedback mechanism to tune down Hh signaling activity. In addition, we provide evidence that Gli proteins are regulated by HIB in a fashion similar to Ci and that downregulation of Ci activity posterior to the MF is essential for normal eye development.
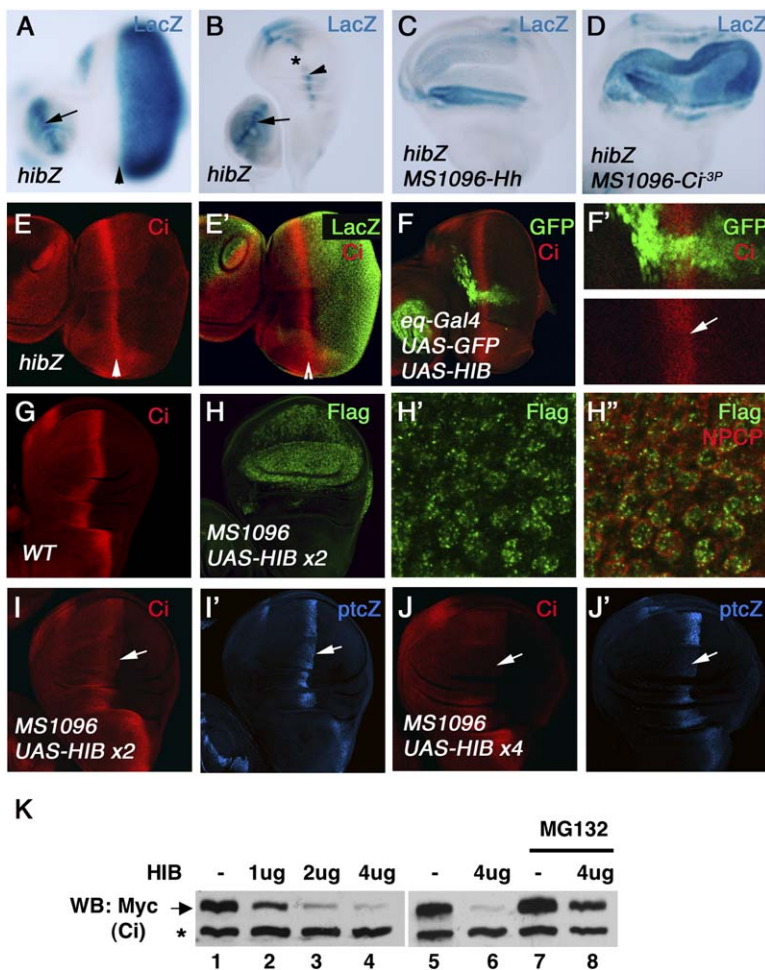
Results

HIB Is a Hh-Induced BTB Protein Expressed Posterior to the MF

Unlike other species that have multiple MATH/BTB domain containing proteins, Drosophila has only one MATH/BTB protein, which is encoded by CG9924 (Stogios et al., 2005). We identified a CG9924 enhancer trap line (l(3)03477) that expresses lacZ in eye discs specifically posterior to the MF (Figures 1A, 1E, and 1E′). We examined the expression pattern of endogenous CG9924 transcription by in situ hybridization and found that it coincides with the lacZ expression pattern derived from l(3)03477 (Figure S1C). Interestingly, l(3)03477-lacZ and CG9924 transcript are both elevated near the anterior-posterior (A/P) compartment boundary

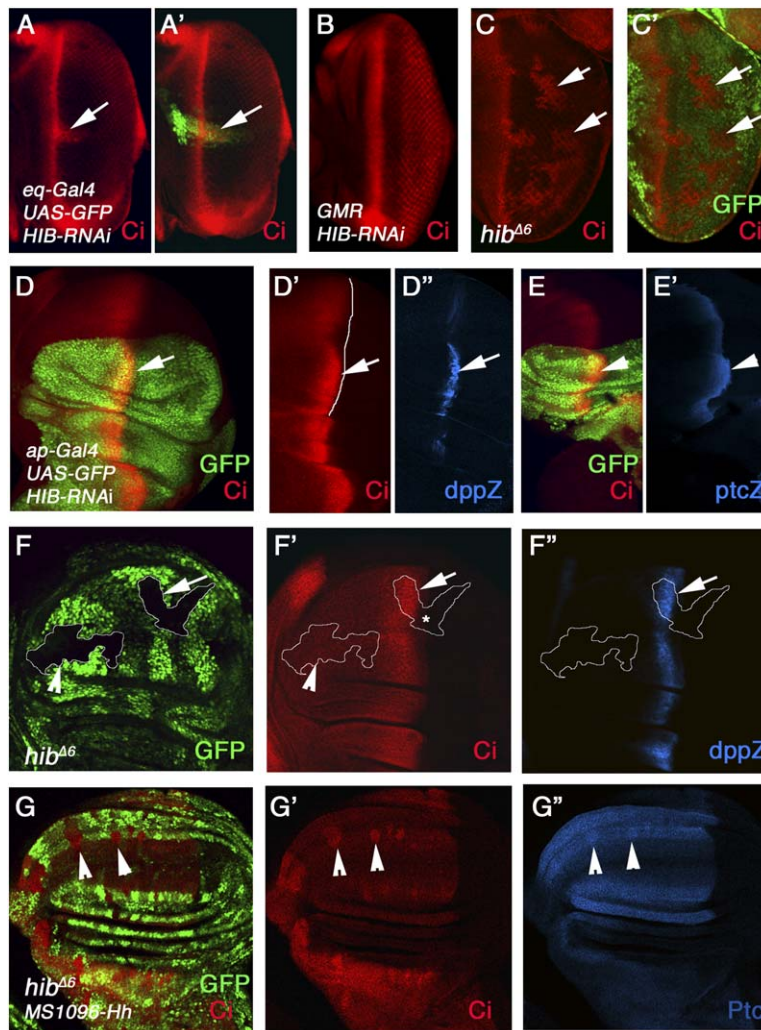**Figure 1. HIB Downregulates Ci[FL] through Proteasome**

(A–D) *LacZ* expression from a HIB enhancer trap line, *l(3)03477* (*hib-Z*), in eye-antenna disc (A), wing and leg discs (B), or wing discs expressing *UAS-Hh* (C) or *UAS-HA-Ci[-3P]* (D) with *MS1096*. *hib-lacZ* is restricted posterior to the MF of eye discs (arrowhead in [A]) and is elevated along the A/P compartment border in antenna (arrow in [A]), wing (arrowhead in [B]), and leg (arrow in [B]) discs. Misexpression of Hh induces ectopic *hib-lacZ* expression in A compartment cells (C), whereas Ci[-3P] induces ectopic *hib-lacZ* expression in both A and P compartments (D). Of note, *hib-lacZ* expression is downregulated near the dorsal-ventral compartment boundary in the wing disc (asterisk).

(E and E′) An eye-antenna disc immunostained to show Ci[FL] (red) and *hib-lacZ* (green) expression. *hib-lacZ*-expressing cells have diminished levels of Ci[FL].

(F and F′) An eye-antenna disc expressing *UAS-GFP* plus multiple copies of *UAS-Flag-HIB* with *eq-Gal4* was immunostained to show GFP (green) and Ci[FL] (red) expression. GFP marks the cells expressing HIB transgenes. Misexpression of HIB resulted in a reduction of Ci[FL] at the MF (arrow in [F′]).

(G–J′) Wild-type wing disc (G) and wing discs expressing two copies (H–H″, I, and I′) or four copies (J and J′) of *UAS-Flag-HIB* were immunostained to show the expression of Ci[FL] (red in [G], [I], and [J]), Flag (green in [H]–[H″]), *ptc-lacZ* (blue in [I′] and [J′]), and a nuclear pore complex protein (NPCP, red in [H″]). Overexpressing HIB caused downregulation of Ci[FL] at the A/P boundary (arrows in [I] and [J]) and a reduction of *ptc-lacZ* expression (arrows in [I′] and [J′]). Flag-HIB exhibited punctate staining in the nuclei encircled by the NPCP staining (H′ and H″). Of note, *MS1096* expresses Gal4 at higher levels in the dorsal compartment than in the ventral compartment (H).

(K) S2 cells were transfected with 6 μg Myc-Ci and indicated amounts of Flag-HIB expression construct, and treated with or without MG132, followed by Western blot analysis. The arrow indicates Myc-Ci, and the asterisk indicates a nonspecific band that serves as a loading control.

of antenna, leg, and wing discs (Figures 1A and 1B; Figures S1C and S1D), suggesting that *CG9924* transcription is induced by Hh signaling and may regulate Hh signaling in multiple tissues. Indeed, misexpressing Hh or an active form of Ci (Ci[-3P]; Wang et al., 1999) in wing disc resulted in ectopic *CG9924* expression (Figures 1C and 1D; Supplementary Figures 1E and 1F). Hence, we name this protein HIB for *H*h-*i*nduced MATH and *B*TB domain protein.

HIB Promotes Ci Degradation in a Proteasome-Dependent Manner

To determine whether HIB regulates Ci[FL] abundance, we misexpressed HIB across the MF using the equator *gal4* driver, *eq-Gal4* (Ou et al., 2002). HIB is restricted posterior to the MF where Ci[FL] level is low in wild-type eye disc (Figures 1A, 1E, and 1E′). We found that misexpression of HIB across the MF reduced Ci[FL] accumulation at the MF (Figures 1F and 1F′), suggesting that HIB is a rate-limiting factor that downregulates Ci[FL] in the eye disc. Likewise, overexpressing HIB in wing discs using the *MS1096 gal4* driver diminished Ci[FL] accumulation near the A/P compartment boundary and inhibited Hh signaling, as indicated by a reduction of the Hh pathway target

ptc-lacZ (Figures 1I and 1I′). Increasing the dose of HIB resulted in more dramatic blockage of Ci[FL] accumulation and *ptc-lacZ* expression (Figures 1J and 1J′). In cultured *Drosophila* S2 cells, coexpression of HIB with Ci[FL] also downregulated Ci[FL] levels in a dose-dependent manner, and this downregulation was inhibited by treatment with the proteasome inhibitor MG132 (Figure 1K), suggesting that HIB promotes degradation of Ci[FL] through the proteasome.

Loss of HIB Results in Elevation of Ci[FL] and Hh Pathway Activity

To determine whether HIB is required for Ci[FL] instability in eye discs posterior to the MF or in wing discs near the A/P boundary, we employed the heritable RNAi technique to inactivate HIB (Kennerdell and Carthew, 2000). Expressing a HIB RNAi construct (*UAS-HIB-RNAi*) in eye discs with either *eq-Gal4* or *GMR-Gal4* led to an elevation of Ci[FL] posterior to the MF (Figures 2A and 2B). *UAS-HIB-RNAi* expression in the dorsal compartment of wing discs using *apterous-Gal4* (*ap-Gal4*) also resulted in elevation of Ci[FL] and Hh pathway activity, as manifested by increased expression of *dpp-lacZ* and *ptc-lacZ* (Figures 2D–2E′), suggesting that HIB

Figure 2. Loss of HIB Results in Elevation of Ci^{FL} and Hh Signaling Activity

(A–B) Eye discs expressing multiple copies of *UAS-HIB-RNAi* plus *UAS-GFP* with *eq-Gal4* (A and A′) or *GMR-Gal4* (B) were immunostained with Ci^{FL} (red) and GFP (green) antibodies. HIB knockdown resulted in Ci^{FL} elevation posterior to the MF.

(C and C′) $hib^{\Delta 6}$ clones were generated in eye disc, followed by immunostaining with GFP (green) and Ci (red) antibodies. Ci^{FL} is accumulated in posterior $hib^{\Delta 6}$ clones (marked by the lack of GFP expression and indicated by arrows).

(D–E′) Wing discs expressing multiple copies of *UAS-HIB-RNAi* plus *UAS-GFP* with *ap-Gal4* were immunostained to show the expression of Ci^{FL} (red in [D], [D′], and [E]), GFP (green in [D] and [E]), and *dpp-lacZ* (D″) or *ptc-lacZ* (E′). GFP marks the cells expressing *UAS-HIB-RNAi*, and the white line in D′ traces the A/P border. HIB knockdown leads to elevation of Ci^{FL} and enhanced expression of *dpp-lacZ* and *ptc-lacZ* near the A/P border.

(F–F″) A wing disc carrying $hib^{\Delta 6}$ clones was immunostained to show the expression of Ci^{FL} (red), GFP (green), and *dpp-lacZ* (blue). $hib^{\Delta 6}$ clones are recognized by the lack of GFP and outlined by white lines. *hib* mutant cells near the A/P boundary (arrow) exhibit elevated Ci^{FL} and enhanced *dpp-lacZ* expression, whereas *hib* mutant cells distant from the A/P boundary show little or no change in Ci^{FL} level (arrowhead). Of note, *hib* mutant cells close to the D/V boundary failed to accumulate Ci^{FL} (asterisk).

(G–G″) A wing disc carrying $hib^{\Delta 6}$ clones and expressing *MS1096/UAS-Hh* was immunostained with Ci^{FL} (red), GFP (green), and Ptc (blue) antibodies. Misexpression of Hh in A compartment cells induced activation but instability of Ci^{FL}; however, A compartment *hib* mutant cells (marked by the lack of GFP and indicated by arrowheads) stabilized the Ci^{Act} and exhibited enhanced Ptc expression regardless of their positions along the A/P axis.

normally attenuates Hh signaling by downregulating Ci^{FL} in A compartment cells near the A/P boundary.

l(3)03477 harbors a P element inserted into the second annotated intron of *hib* (Figure S1A), and the associated lethality is reversed by precise excision of the P element. The P element insertion results in a dramatic reduction, but not complete loss, of *hib* expression (Figure S1B). Mutant clones homozygous for *l(3)03477* only exhibited modestly increased Ci^{FL} posterior and close to the MF, whereas *l(3)03477* mutant cells situated in more posterior regions did not exhibit a detectable change in Ci^{FL} level (Figures S3A and S3B). The lack of strong phenotype associated with *l(3)03477* is likely due to the hypomorphic nature of this mutation, as suggested by residual *hib* expression in *l(3)03477* homozygotes (Figure S1B). Indeed, posterior mutant clones homozygous for a *hib* deficiency, *Df(3R)Exel6171*, accumulated high levels of Ci^{FL} posterior to the MF in regions both close to and distant from the MF (Figures S3C and S3D).

To further explore the role of HIB in the Hh pathway, we generated a null mutation by "ends-out" gene targeting in which *hib* coding sequence was replaced by the *white* gene (Gong and Golic, 2003). Two independent targeting alleles, $hib^{\Delta 6}$ and $hib^{\Delta 14}$, were isolated (Figure S2) and exhibited similar phenotypes (data not shown). We used $hib^{\Delta 6}$ to carry out all the following experiments.

$hib^{\Delta 6}$ mutant clones posterior to the MF accumulated high levels of Ci^{FL} similar to *Df(3R)Exel6171* (Figures 2C and 2C′; Figures S3C–S3F), confirming that $hib^{\Delta 6}$ is a null allele. In wing discs, $hib^{\Delta 6}$ mutant clones located near the A/P boundary exhibited elevated Ci^{FL} and enhanced *dpp-lacZ* expression (Figures 2F–2F″). In contrast, A compartment $hib^{\Delta 6}$ mutant clones distant from the A/P boundary did not affect Ci^{FL}, suggesting that HIB targets Ci^{FL} in Hh-receiving cells. To further test this hypothesis, we misexpressed Hh uniformly in wing pouch regions carrying $hib^{\Delta 6}$ mutant clones. Misexpressing Hh in A compartment cells converts Ci^{FL} into active but labile forms, as manifested by ectopic *ptc* expression and diminished Ci^{FL}; however, Ci^{FL} is stabilized in anteriorly situated $hib^{\Delta 6}$ mutant clones (Figures 2G and 2G′). Moreover, the level of ectopic *ptc* is higher in $hib^{\Delta 6}$ mutant cells than in neighboring hib^+ cells (Figure 2G″),
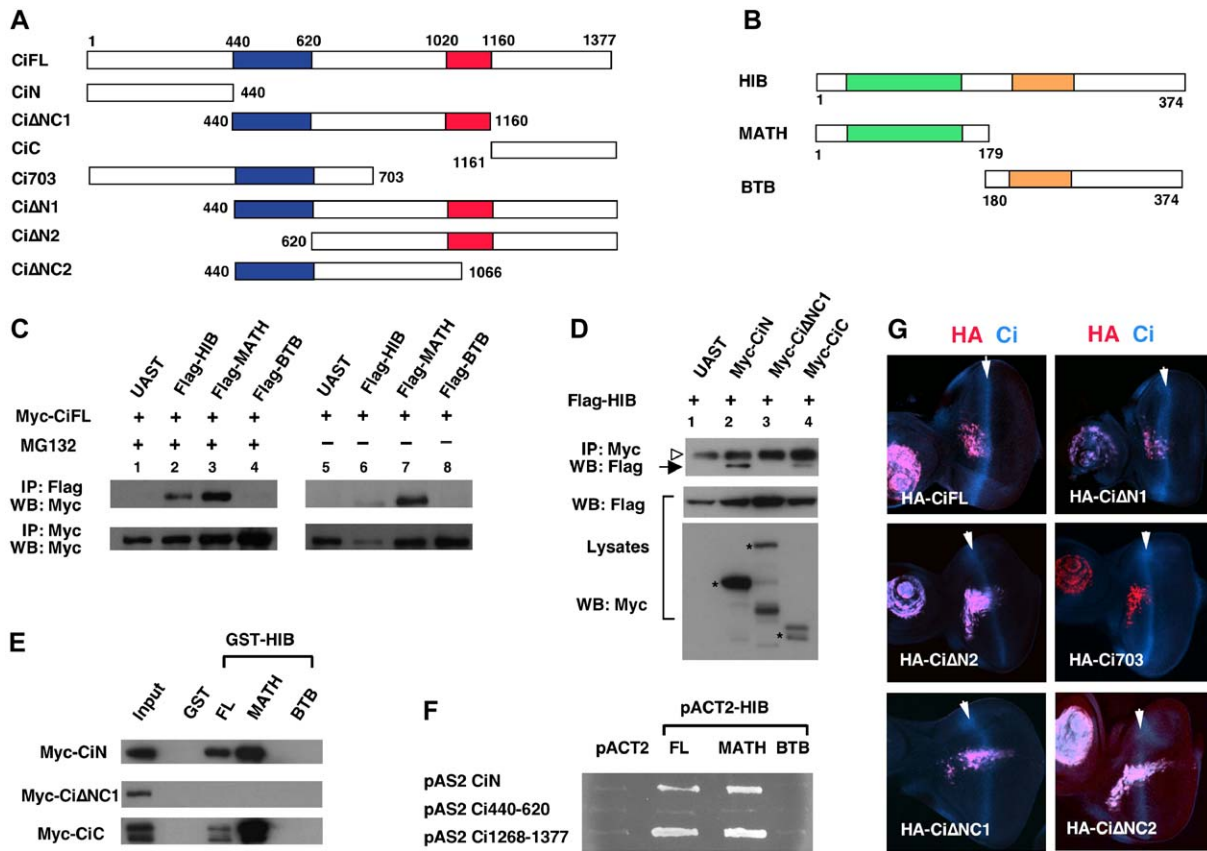
Figure 3. Both the N- and C-Terminal Regions of Ci Bind the MATH Domain of HIB and Target Ci for Degradation

(A and B) Schematic drawings of Ci and HIB and their deletion mutants. Blue and red bars indicate the Zn finger DNA binding and dCBP binding domains of Ci. Green and orange bars denote the MATH and BTB domains of HIB.

(C) Western blots (WB) of immunoprecipitates (IP) from S2 cells expressing indicated proteins and treated with (+) or without (−) MG132.

(D) Western blots of immunoprecipitates (top) or lysates (bottom two panels) from S2 cells expressing indicated proteins and treated with MG132. The arrow indicates Flag-HIB coimmunoprecipitated with Myc-CiN or Myc-CiC. The open arrowhead indicates IgG. Asterisks indicate expressed Ci deletion mutants.

(E) Extracts from S2 cells expressing indicated Myc-tagged Ci mutants were incubated with GST or indicated GST fusion proteins. The bound proteins were analyzed by Western blot with Myc antibody. Equal amounts of GST and GST fusion proteins were used.

(F) pAS2 Ci deletion constructs were transformed into yeast with indicated pACT2 HIB constructs, and transformants were grown on selection media.

(G) Eye discs expressing indicated HA-tagged Ci deletion mutants with *eq-Gal4* were immunostained with HA (red) and Ci (blue) antibodies. The MF is demarcated by the elevation of endogenous Ci (arrowheads). Of note, HA-Ci703 was not stained by the anti-Ci antibody, which recognizes a C-terminal region epitope deleted from Ci703 (Motzny and Holmgren, 1995).

suggesting that HIB attenuates Hh signaling outputs by downregulating the active forms of Ci^{FL}.

Of note, *hib*$^{\Delta6}$ mutant cells near the junction between the A/P and D/V boundaries did not accumulate Ci^{FL} (indicated by an asterisk in Figure 2F′). One possibility is that perdurance of residual HIB in *hib* mutant cells could be responsible for Ci degradation in this region. Alternatively, a HIB-independent mechanism might act redundantly with HIB to degrade active forms of Ci in response to high levels of Hh.

HIB Promotes Ci Degradation by Binding to Its N- and C-Terminal Domains

The N- and C-terminal regions of HIB contain a MATH and a BTB domain, respectively (Figure 3B). Several recent studies revealed that BTB domain-containing proteins interact with Cul3 through their BTB domains and function as substrate recognition subunits for Cul3-based E3 ubiquitin ligases (Pintard et al., 2004). Therefore, we carried out biochemical experiments to assess whether HIB interacts with Ci and Cul3. Coimmunoprecipitation (CoIP) experiments showed that Myc-tagged full-length Ci (Myc-Ci^{FL}) formed a complex with Flag-tagged HIB (Flag-HIB) in S2 cells; however, a stable complex was detected only when S2 cells were treated with the proteasome inhibitor MG132 (Figure 3C, compare lanes 2 and 6), consistent with the observation that HIB promotes proteasome-dependent Ci^{FL} degradation (Figure 1K). In contrast, the N-terminal HIB fragment containing the MATH domain (Flag-MATH) formed a stable complex with Myc-Ci^{FL} regardless of MG132 treatment (Figure 3C, compare lanes 3 and 7), whereas the C-terminal fragment containing the BTB domain (Flag-BTB) failed to bind Myc-Ci^{FL} (Figure 3C, lanes 4 and 8).

To map the HIB-interacting domain(s) in Ci, Myc-tagged Ci deletion mutants were transfected into S2 cells with Flag-HIB, followed by CoIP. As shown in Figure 3D, both the N- and C-terminal Ci fragments
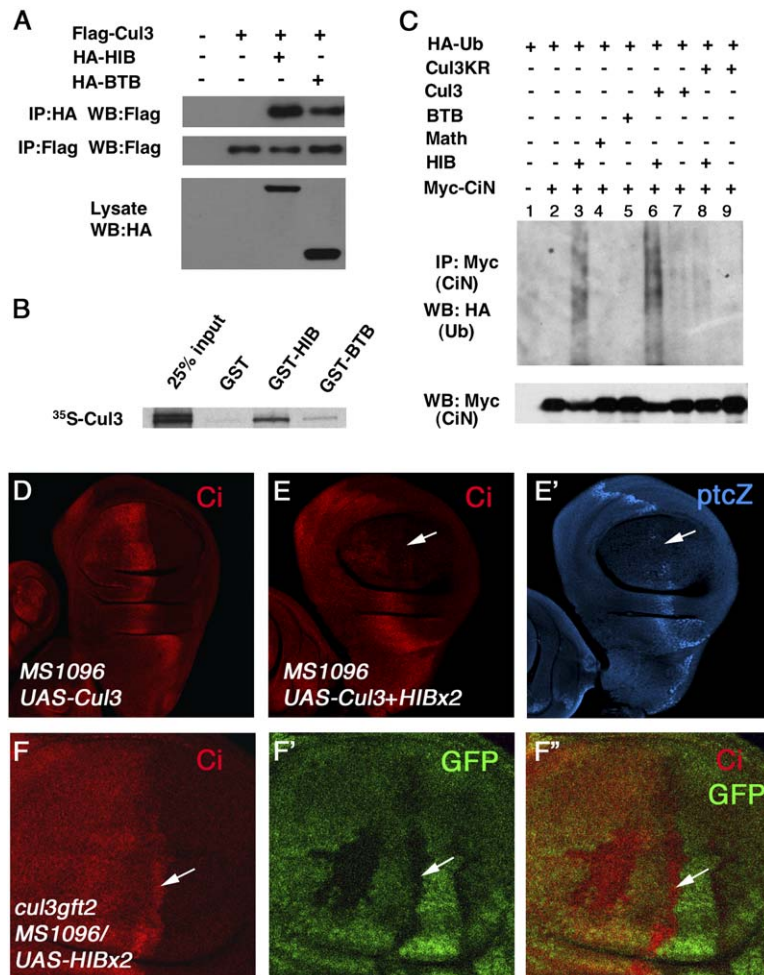
Figure 4. HIB Interacts with Cul3 to Promote Ci Ubiquitination and Degradation

(A) Western blots of immunoprecipitates (top panels) or lysates (bottom panel) from S2 cells expressing the indicated proteins.

(B) Autoradiogram of in vitro translated and ^{35}S-labeled Cul3 bound to GST-HIB or GST-BTB. Equal amounts of GST and GST fusion proteins were used.

(C) In vivo ubiquitination of CiN promoted by HIB. Myc-CiN was immunoprecipitated from S2 cells expressing the indicated proteins and treated with MG132, followed by Western blot with HA antibody to detect conjugated HA-Ub. Roc1a was also included in the transfection (not shown). Cell lysates were immunoblotted with Myc antibody to monitor the level of Myc-CiN (bottom panel). Loading was normalized according to Myc-CiN level.

(D–E′) Wing discs overexpressing Cul3 alone (D) or Cul3 plus HIB (E and E′) were immunostained to show the expression of Ci^{FL} (red) and *ptc-lacZ* (blue). Coexpression of Cul3 with HIB resulted in more dramatic downregulation of Ci^{FL} near the A/P boundary (arrow in [E]; compare with Figure 1I) and more complete blockage of *ptc-lacZ* expression (arrow in [E′]; compare with Figure 1I′).

(F–F″) A wing disc carrying *cul3^{gft2}* clones and expressing two copies of *UAS-Flag-HIB* with *MS1096* were immunostained to show the expression of Ci^{FL} (red) and GFP (green). *cul3* mutant cells are marked by the lack of GFP expression. *cul3* mutant cells near the A/P boundary accumulated high levels of Ci even when HIB was overexpressed (arrows).

(Myc-CiN and Myc-CiC) pulled down Flag-HIB, whereas the middle region of Ci containing the Zn finger DNA binding domain and dCBP binding domain (Myc-CiΔNC1) showed little or no interaction with Flag-HIB. GST pull-down experiments confirmed that both CiN and CiC interact with HIB through the MATH domain (Figure 3E). Finally, both HIB-FL and MATH, but not BTB, interact with the N- and C-terminal regions of Ci in yeast (Figure 3F), demonstrating that HIB directly binds two distinct domains of Ci through its MATH domain.

To assess whether the HIB-interacting domains mediate Ci degradation in vivo, we expressed various HA-tagged Ci deletion mutants lacking either the N-terminal (HA-CiΔN1 and HA-CiΔN2) or the C-terminal (HA-Ci703) HIB binding domain, or both (HA-CiΔNC1 and HA-CiΔNC2) in eye discs with *eq-Gal4*. Ci mutants lacking either the N- or C-terminal HIB binding domain were still degraded posterior to the MF; however, Ci mutants lacking both HIB binding domains were stabilized (Figure 3G), suggesting that either the N- or the C-terminal domain alone can target Ci^{FL} for HIB-mediated degradation.

HIB Forms a Complex with Cul3 and Promotes Ci Ubiquitination and Degradation through Cul3

To determine whether HIB forms a complex with Cul3, S2 cells were transfected with Flag-tagged Cul3 plus HA-tagged full-length HIB (HA-HIB) or its BTB-containing fragment (HA-BTB). As shown in Figure 4A, Flag-Cul3 was coimmunoprecipitated with both HA-HIB and HA-BTB. In addition, in vitro translated Cul3 was specifically pulled down by GST-HIB or GST-BTB (Figure 4B), suggesting that HIB interacts with Cul3 through its BTB domain.

To determine whether HIB promotes Ci^{FL} degradation through Cul3, we overexpressed HIB in wing discs carrying *cul3* mutant clones. HIB failed to downregulate Ci^{FL} in *cul3* mutant cells near the A/P boundary (Figures 4F–4F″). On the other hand, coexpressing Cul3 with HIB facilitated Ci^{FL} degradation at the A/P boundary (Figure 4E), leading to near complete blockage of *ptc-lacZ* expression (Figure 4E′). Of note, overexpression of Cul3 alone slightly stabilized Ci^{FL} in A compartment cells both close to and distant from the A/P compartment boundary (Figure 4D), likely due to a squelching effect whereby excess amounts of Cul3 titrated out other components (such as BTB protein or Roc1) of the E3 ligase, thus interfering with the assembly of functional E3 ligase complexes.

To determine whether a HIB-Cul3 complex promotes Ci ubiquitination, we carried out an in vivo ubiquitination assay (see Experimental Procedures). As shown in Figure 4, HIB promotes CiN ubiquitination in S2 cells, likely through endogenous Cul3 (Figure 4C, lane 3).
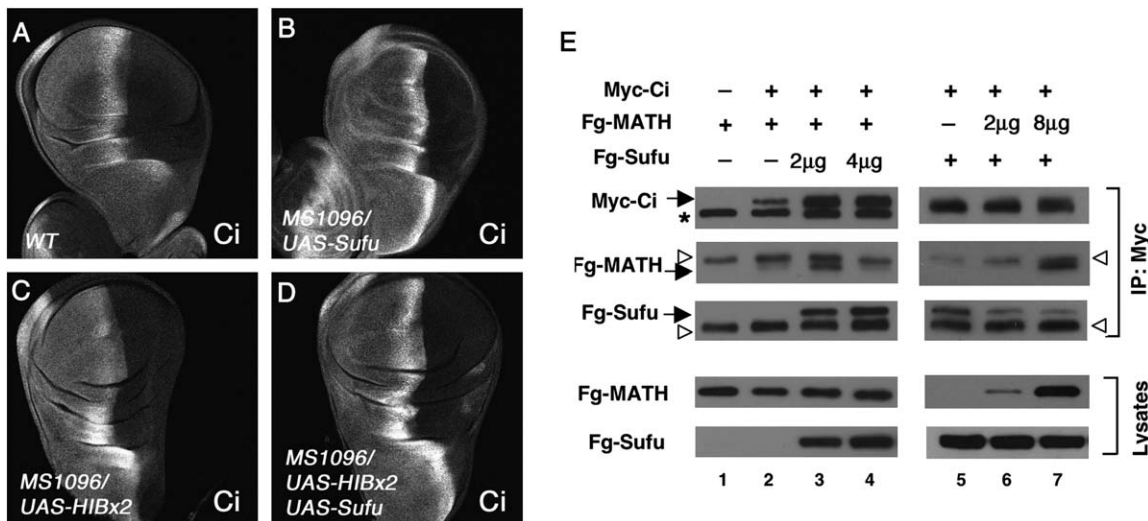
Figure 5. Sufu Interferes with HIB-Mediated Ci Degradation

(A–D) Ci^{FL} expression in a wild-type wing disc (A) or wing discs expressing *UAS-Myc-Sufu* (B), two copies of *UAS-Flag-HIB* (C), or two copies of *UAS-Flag-HIB* plus *UAS-Myc-Sufu* (D) with *MS1096*.
(E) Sufu and MATH compete for binding to Ci. S2 cells were transfected with Myc-Ci together with fixed amount of Flag-MATH and increasing amounts of Flag-Sufu (lanes 3–4) or fixed amount of Flag-Sufu and increasing amounts of Flag-MATH (lanes 6 and 7). Cell lysates were immunoprecipitated with Myc antibody and immunoblotted with Myc or Flag antibody (top panels). Cell lysates were also directly immunoblotted with Flag antibody (bottom panels). Open arrowheads indicate IgG, and the asterisk indicates a nonspecific band.

Cotransfection of a dominant-negative form of Cul3, Cul3^{KR} (Wu et al., 2005), reduced HIB-mediated CiN ubiquitination (Figure 4C, lane 8), whereas coexpression of a wild-type Cul3 enhanced CiN ubiquitination (Figure 4C, lane 6). Consistent with HIB bridging Ci with Cul3, the HIB MATH or BTB domain alone failed to induce CiN ubiquitination (Figure 4C, lanes 4 and 5) or suppress Ci^{FL} accumulation in *hib^{Δ6}* cells (Figures S4B and S4C). Moreover, overexpressing MATH in wing discs stabilized Ci^{FL} near the A/P boundary (data not shown), suggesting that the MATH domain alone behaves in a dominant-negative fashion.

Sufu Protects Ci from HIB-Mediated Degradation

Hh stimulates the maturation of Ci^{FL} into a short-lived nuclear transcriptional activator, whereas Sufu opposes this step by interacting with Ci^{FL} (Ohlmeyer and Kalderon, 1998). Indeed, mutations in Sufu increase Hh target gene expression but destabilize Ci^{FL} (Ohlmeyer and Kalderon, 1998). Conversely, overexpressing Sufu stabilized Ci^{FL} near the A/P compartment boundary (compare Figures 5A and 5B). We noticed that like HIB, Sufu also binds both the N- and C-terminal regions of Ci (Methot and Basler, 2000; Monnier et al., 1998; Q.Z. and J.J., unpublished data), raising the possibility that Sufu binding may stabilize Ci^{FL} by excluding HIB. We therefore carried out experiments to determine whether Sufu and HIB bind competitively to Ci^{FL}. As shown in Figure 5E, increasing the amount of Sufu diminished the amount of MATH immunoprecipitated by Ci^{FL} and vice versa. In wing discs, coexpressing Sufu prevents Ci^{FL} degradation induced by overexpressed HIB (Figure 5D). Hence, Ci^{Act}, which presumably dissociates from Sufu, becomes short-lived because it is more accessible to HIB-mediated degradation.

Loss of HIB Enhances the Overgrowth Caused by an Activated Form of Ci

Hh prevents Ci phosphorylation (Chen et al., 1999; Zhang et al., 2005), which not only blocks Slimb-mediated proteolysis but also contributes to the activation of Ci^{FL} (Wang et al., 1999). Our finding that HIB downregulates Ci^{Act} in Hh-receiving cells implies that it may promote Ci degradation independent of Ci phosphorylation. Indeed, Ci^{-3P}, which lacks three PKA sites in its C-terminal region and thus is unable to undergo sequential phosphorylation by PKA, GSK3, and CKI, is still degraded by HIB in eye discs posterior to the MF (Figures 6A–6A″). Misexpression of Ci^{-3P} in wing discs activated Hh target genes in both A and P compartments and caused enlargement of wing discs due to overgrowth (Figure 6C). Removal of HIB in wing discs expressing Ci^{-3P} greatly enhanced the overgrowth phenotype (compare Figure 6D to Figure 6C). Strikingly, *hib* mutant cells expressing Ci^{-3P} formed tumor-like overgrowths (Figures 6D and 6E). In addition, *hib* mutant cells accumulated higher levels of Ci^{-3P} (Figures 6E and 6E′) and exhibited enhanced Hh pathway activation, as indicated by higher levels of ectopic Ptc (Figure 6E″). Hence, loss of *hib* synergizes with Ci^{-3P} to induce wing overgrowth.

HIB is Localized in the Nucleus

Our data so far suggest that HIB can target the active forms of Ci for degradation. As Ci^{Act} is thought to act in the nucleus, we went on to examine whether HIB also resides in the nucleus. We expressed Flag-HIB either in wing discs or eye discs posterior to the MF and monitored the subcellular localization of HIB by immunostaining with a Flag antibody. We marked the nuclei with either anti-Elav antibody, which stains the nuclei of differentiating neurons in eye discs, or anti-NPCP
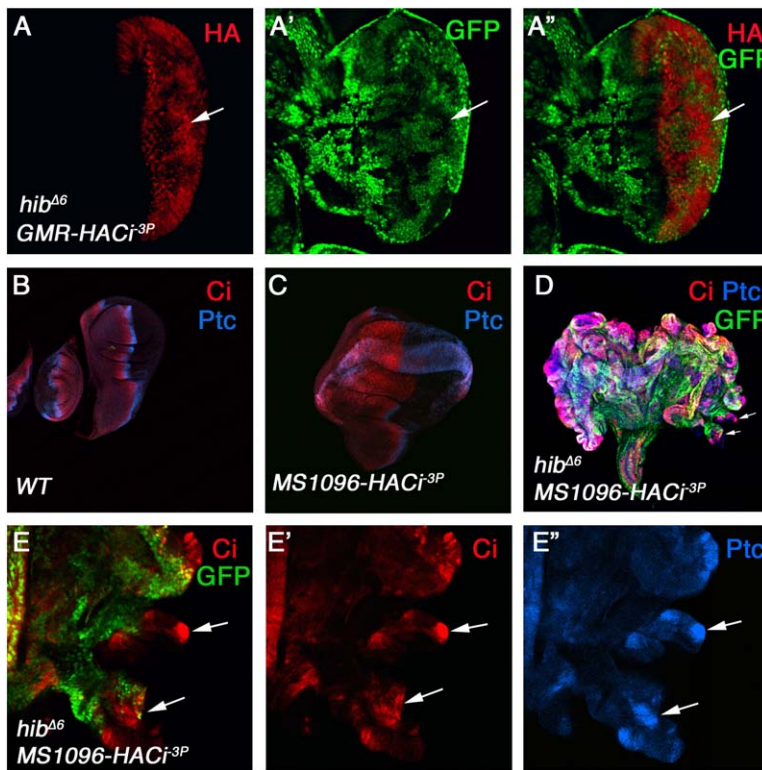
Figure 6. HIB Regulates the Activity of a Phosphorylation-Deficient Form of Ci

(A–A″) $hib^{\Delta 6}$ clones were produced in eye disc expressing *UAS-HA-Ci^{-3P}* with *GMR-Gal4*, followed by immunostaining with GFP (green) and HA (red) antibodies. HA-Ci^{-3P} was stabilized in *hib* mutant cells marked by the lack of GFP (arrows).

(B and C) Low magnification view of wild-type (B) or *MS1096/UAS-HA-Ci^{-3P}* (C) wing disc immunostained with Ci (red) and Ptc (blue) antibodies. HA-Ci^{-3P} induced ectopic Ptc and disc overgrowth.

(D–E″) Low (D) and high (E–E″) magnification views of a wing disc expressing *MS1096/UAS-HA-Ci^{-3P}* and carrying $hib^{\Delta 6}$ clones marked by the lack of GFP. P compartment $hib^{\Delta 6}$ clones expressing HA-Ci^{-3P} accumulated higher levels of Ci^{-3P}, expressed higher levels of Ptc than neighboring hib^+ cells, and protruded out from the epithelia layer (arrows).

antibody, which recognizes a nuclear pore complex protein. As shown in Figures 1H–1H″ and Figure S5, Flag-HIB exhibited punctate staining mainly in the nucleus in both wing and eye discs. A similar subcellular localization has been observed for the mammalian homolog of HIB (Kwon et al., 2006). Hence, the subcellular localization of HIB suggests that HIB promotes ubiquitination and degradation of Ci in the nucleus.

**HIB/SPOP Regulates Degradation of Gli Proteins**

The regulation of Ci/Gli in Hh signaling is largely conserved between *Drosophila* and vertebrates (Jia and Jiang, 2006). There are multiple HIB homologs in vertebrates (Figure S1G). Mouse SPOP protein shares 79% amino acid sequence identity with HIB. To determine whether SPOP can degrade Ci in place of HIB, we expressed SPOP in eye discs carrying *hib* mutant clones. We found that *hib* mutant clones posterior to the MF no longer accumulated high levels of Ci^{FL} when they expressed SPOP (Figures 7A–7A″), suggesting that SPOP degrades Ci^{FL} in the absence of HIB.

To further explore whether HIB/SPOP represents a conserved regulator of the Ci/Gli family of transcription factors, we tested whether Gli proteins could be degraded by HIB/SPOP in a way similar to Ci. Gli2 and Gli3 are the primary transcriptional effectors of the vertebrate Hh signaling pathway (Jia and Jiang, 2006; Stamataki et al., 2005). When expressed in eye discs with *eq-Gal4*, both Gli2 and Gli3 were selectively degraded posterior, but not anterior, to the MF (Figures 7B and 7C). To determine whether HIB is responsible for degrading Gli proteins posterior to the MF, we expressed Gli2 and Gli3 in eye discs carrying *hib* mutant clones. Indeed, both Gli2 and Gli3 were stabilized in *hib* mutant cells posterior to the MF, as was the case for Ci^{FL} (Figures 7D–7E′). Furthermore, expressing SPOP blocked the accumulation of Gli proteins in *hib* mutant clones (data not shown). When expressed in the wing disc, Gli2 accumulated at higher levels and induced higher levels of Ptc in *hib* mutant cells than in neighboring hib^+ cells (Figures 7F–7G″). Taken together, these observations strongly argue that HIB/SPOP plays a conserved role in Ci/Gli degradation.

Downregulation of Ci Activity by HIB Is Essential for Eye Development

Hh is expressed posterior to the MF; however, Hh-responsive genes are only turned on near the MF but not in the differentiating cells posterior to the MF. It is possible that Hh pathway activity needs to be turned off in differentiating cells in order for their normal development, and degradation of Ci by HIB may provide a mechanism to prevent aberrant Hh pathway activity. To test this hypothesis, we misexpressed either the full-length (Ci^{FL}) or truncated forms of Ci lacking either one (CiΔN1) or both (CiΔNC1) HIB binding domains in eye discs posterior to the MF. Misexpression of Ci^{FL} did not lead to abnormal eye morphology within the resolution of light microscopy (compare Figure 7I to Figure 7H); however, misexpression of either CiΔN1 or CiΔNC1 caused eye roughness, with CiΔNC1 causing a more severe phenotype (Figures 7J and 7K). Although misexpressing Ci^{FL} alone did not significantly perturb eye development, misexpressing Ci^{FL} in eye discs carrying *hib* mutant clones resulted in severe rough eye phenotype (Figure 7M). Similarly, misexpressing Ci^{-3P} and Gli2 in eye discs carrying *hib* mutant clones also caused severe rough eye phenotype (Figures 7N and 7O), whereas misexpressing Ci^{-3P} and Gli2 in otherwise wild-type eye discs failed to do so (data not shown). Taken together, these results
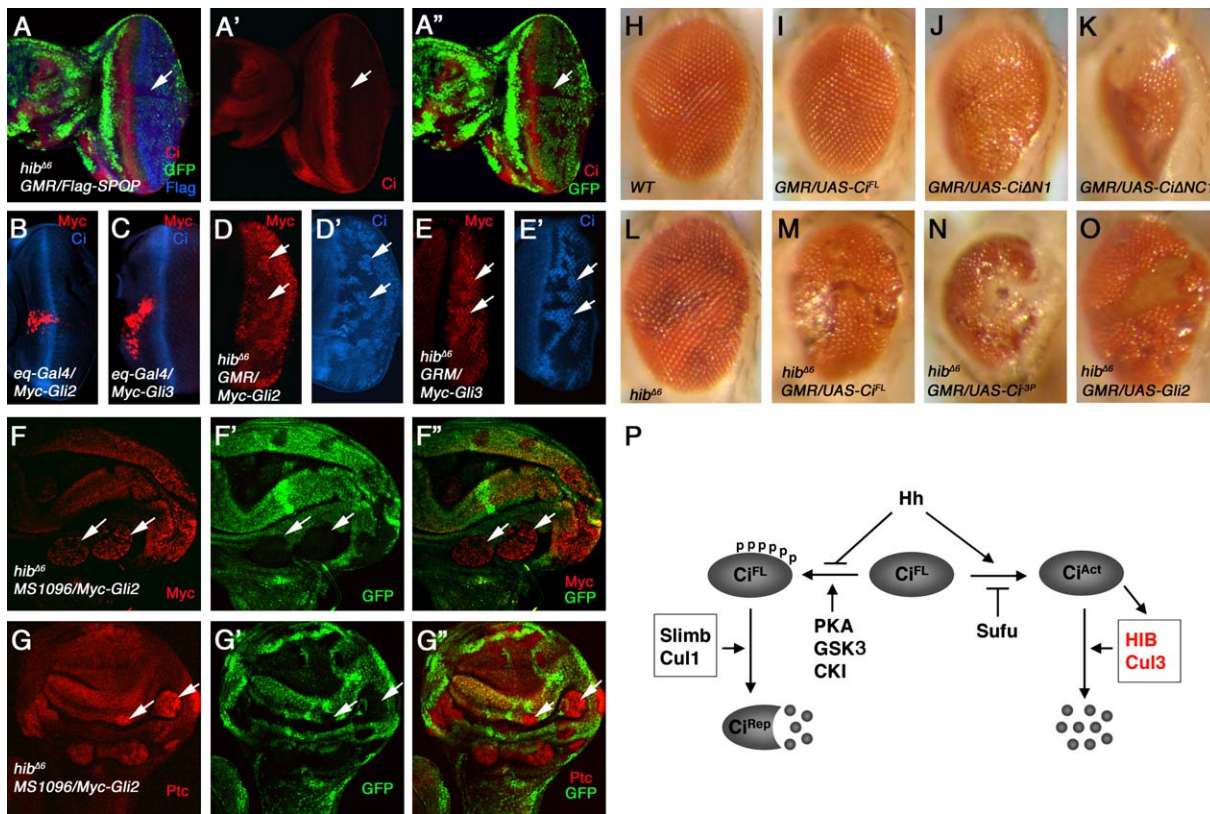
Figure 7. Downregulation of Ci/Gli by HIB/SPOP Prevents Aberrant Hh Pathway Activity Posterior to the MF, which Is Essential for Normal Eye Development

(A–A″) Flag-SPOP (blue) was expressed in an eye disc carrying $hib^{\Delta 6}$ clones marked by the lack of GFP expression (green). SPOP blocked Ci^{FL} (red) accumulation in hib mutant cells posterior to the MF (arrows).

(B and C) Eye discs expressing Myc-Gli2 (B) or Myc-Gli3 (C) with eq-$Gal4$ were immunostained with Myc (red) and Ci (blue) antibodies. Both Myc-Gli2 and Myc-Gli3 are degraded posterior to the MF, which is marked by high levels of Ci^{FL}.

(D–E′) Myc-Gli2 (D and D′) or Myc-Gli3 (E and E′) was expressed using GMR-$Gal4$ in eye discs carrying $hib^{\Delta 6}$ clones. The discs were immunostained with Myc (red) and Ci (blue) antibodies. Both Myc-Gli2 and Myc-Gli3 were stabilized in $hib^{\Delta 6}$ clones, which are marked by Ci^{FL} elevation (arrows).

(F–G″) $hib^{\Delta 6}$ clones were induced in wing discs expressing $MS1096/UAS$-Myc-$Gli2$, followed by immunostaining with GFP (green), Myc (red in [F] and [F″]), and Ptc (red in [G] and [G″]) antibodies. hib mutant cells (arrows) accumulated higher levels of Myc-Gli2 and expressed higher levels of Ptc than neighboring hib^+ cells.

(H–K) Wild-type (H) adult eye or adult eyes expressing GMR-$Gal4/UAS$-Ci^{FL} (I), GMR-$Gal4/UAS$-$Ci\Delta N1$ (J), or GMR-$Gal4/UAS$-$Ci\Delta NC1$ (K).

(L–O) Adult eyes carrying hib mutant clones alone (L), or carrying hib mutant clones and expressing GMR-$Gal4/UAS$-Ci^{FL} (M), GMR-$Gal4/UAS$-Ci^{-3P} (N), or GMR-$Gal4/UAS$-$Gli2$ (O).

(P) A model for regulating Ci by dual ubiquitination systems. In the absence of Hh, Ci^{FL} undergoes sequential phosphorylation by PKA, GSK3, and CKI. Hyperphosphorylation recruits Slimb-Cul1-based E3 ligase that promotes proteolytic processing of Ci^{FL} to generate C-terminally truncated Ci^{Rep}. Hh prevents Ci phosphorylation and induces maturation of Ci^{FL} into Ci^{Act}. Ci^{Act} activates Hh target genes and HIB. HIB-Cul3-based E3 ligase binds Ci^{Act} and promotes its ubiquitination, followed by proteasome-mediated degradation. Sufu opposes the conversion of Ci^{FL} into Ci^{Act} and stabilizes Ci by blocking HIB-Ci interaction.

suggest that failure to degrade Ci by perturbing the HIB activity either in *cis* or in *trans* leads to aberrant Hh signaling and abnormal eye development. We noticed that eye carrying *hib* mutant clones only exhibited mild roughness (Figure 7L), although endogenous Ci was accumulated posterior to the MF. A likely explanation is that additional mechanism(s) may exist to restrict Hh signaling activity posterior to the MF and such a mechanism(s) can be overcome by excess amount of Ci provided exogenously.

Discussion

In this study, we identify HIB as a negative regulator of the Hh pathway and provide genetic and biochemical evidence that HIB is the substrate recognition component of a Cul3-based ubiquitin ligase that binds multiple regions of Ci to catalyze its ubiquitination, followed by proteasome-mediated degradation. Interestingly, Hh induces *hib* transcription, and thus, HIB-mediated downregulation of Ci forms a negative feedback loop to modulate Hh signaling responses. In conjunction with previous studies, our results demonstrate that Ci is regulated by dual ubiquitination systems that act in two distinct signaling states (Figure 7P). In the absence of Hh, the Slimb-Cul1-based ubiquitin ligase targets Ci^{FL} for proteolytic processing to generate Ci^{Rep}, and this process requires prior phosphorylation of Ci^{FL} by PKA, GSK3, and CKI. In the presence Hh, Ci phosphorylation is inhibited and Slimb-Cul1-mediated Ci processing is blocked. Hh further induces nuclear translocation and maturation of Ci^{FL} into Ci^{Act}, which activates Hh target

genes and concomitantly induces the production of HIB. The HIB-Cul3-based E3 ligase then binds and targets Ci^{Act} for ubiquitination and degradation. The subcellular distribution of HIB is consistent with its acting in a nuclear E3 complex that targets nuclear Ci for degradation in Hh responding cells.

Although our observations support the idea that HIB targets Ci^{Act} to downregulate Hh responses, we do not intend to suggest that HIB-Cul3 exclusively regulates Ci^{Act}. As a matter of fact, we find that Ci703, which is similar to Ci^{Rep}, can be degraded by HIB (Figure 3G), raising the possibility that HIB/SPOP could also modulate Hh signaling in certain development contexts, such as vertebrate limb development, that are regulated only by the repressor form of Ci/Gli. Nevertheless, our results do suggest that Ci^{Act} is a better substrate for HIB because (1) it is nuclear and (2) it may dissociate from Sufu or bind Sufu less tightly than latent forms of Ci^{FL}.

Neither do we rule out the possibility that a partially redundant mechanism(s) may exist that targets Ci for degradation in Hh-responding cells. We notice that HIB expression is downregulated near the D/V boundary (Figure 1B) and that *hib* mutant cells near the junction between the A/P and D/V boundaries failed to accumulate Ci^{FL} (Figure 2F′). Although we cannot rule out the possibility that residual HIB in *hib* mutant cells could be responsible for degrading Ci, these observations raise the possibility that a HIB-independent mechanism may exist to degrade Ci^{Act} in response to high thresholds of Hh.

The HIB-Cul3-based regulatory mechanism may provide a means to regulate the strength and/or duration of Hh pathway activity in a spatially or temporally regulated manner. It may also provide a mechanism to terminate Hh signaling in certain developmental contexts, as appears to be the case in *Drosophila* eye development. During *Drosophila* eye development, Hh signaling is required for the initiation and progression of the MF (Treisman and Heberlein, 1998). Although Hh is expressed in differentiating cells posterior to the MF, Hh target genes are not expressed in differentiating cells. We provide evidence that Hh signaling is downregulated through HIB-mediated degradation of Ci posterior to the MF. Furthermore, we demonstrated that termination of Hh signaling posterior to the MF is essential for normal eye development. Indeed, misexpression of truncated forms of Ci that are resistant to HIB-mediated degradation or removal of HIB resulted in rough eye phenotypes (Figures 7H–7O). Hence, during eye development, differentiating cells turn on HIB to prevent aberrant Hh signaling by degrading Ci, which is essential for normal eye development.

The HIB-Cul3-based regulatory mechanism we identify here is likely to be evolutionarily conserved and may play a more general role in fine-tuning Hh responses in various developmental contexts. Indeed, we find that both Gli2 and Gli3, the two primary transcription factors for the vertebrate Hh signaling pathway, are degraded by HIB in a fashion similar to Ci. There are multiple HIB homologs in vertebrates. For example, human and mouse each have two whereas zebrafish has three (Figure S1G). We have demonstrated that mouse SPOP can functionally replace HIB in degrading Ci. It would be interesting to determine whether the other mouse HIB homolog, LOC76857, which shares with SPOP 94% and 83% identical amino acids in their MATH and BTB domains, respectively, can also functionally substitute for HIB, and whether the vertebrate homologs of HIB play any roles in modulating Hh responses in vertebrate development.

A recent study demonstrated that Gli proteins possess dual degradation signals, one regulated by Slimb/β-TRCP-Cu11 E3 ligase and the other by an unknown mechanism (Huntzicker et al., 2006). Moreover, perturbation of Gli degradation mechanisms appears to greatly potentiate the ability of Gli proteins to induce tumor formation in transgenic animals (Huntzicker et al., 2006). Similarly, we found that *hib* mutation greatly enhances the ability of an active form of Ci to induce disc overgrowth (Figure 6D). Our finding that HIB/SPOP also regulates Gli stability raises the exciting possibility that SPOP and its paralogs may act as tumor suppressors whose loss of function could synergize with aberrant Gli activation to induce tumor formation.

We also note that a recent study demonstrated that the Wnt pathway induces a Cul3-based ubiquitin ligase to attenuate pathway activity through degradation of the key pathway component Dishevelled (Angers et al., 2006). Our finding that the Hh pathway also induces a Cul3-based ubiquitin ligase to attenuate pathway activity extends the many interesting parallels between these two pathways (Jia and Jiang, 2006; Kalderon, 2002; Lum and Beachy, 2004) and suggests that similar mechanisms could be employed by other signaling pathways. Given the large number of BTB proteins present in the genomes of various species (Stogios et al., 2005), it should be fruitful to explore the potential roles of BTB-Cul3 E3 ligases in various signaling pathways.

While this manuscript was under review, Kent et al. published a paper online where they made independent observations that CG9924, which they named Roadkill, degrades Ci and attenuates Hh responses (Kent et al., 2006).

Experimental Procedures

Mutations and Transgenes
l(3) 03477, *Df(3R)Exel6171*, *cul3^{gft2}*, *MS1096*, *eq-Gal4*, *ap-Gal4*, *GMR-Gal4*, *UAS-GFP*, *UAS-hh*, *UAS-HA-Ci^{-3P}*, *USA-Ci* deletion mutants, *UAS-Myc-Sufu*, *UAS-Flag-Cul3*, *Myc-Gli2*, *UAS-Myc-Gli3*, *dpp-lacZ*, and *ptc-lacZ* have been described (Flybase; Aza-Blanc et al., 2000; Methot and Basler, 2000; Ou et al., 2002; Wang et al., 1999, 2000). A HIB cDNA clone (RE34508, *Drosophila* DGC2 EST library) was obtained from Open Biosystems. This cDNA clone encodes the B isoform of CG9924 (CG9924-PB; Flybase). To construct *UAS-HIB-RNAi*, a genomic DNA fragment with the coding sequence for HIB amino acids 132–363 was amplified by PCR and cloned into the EcoRI and XhoI sites of *pUAST* vector with the corresponding cDNA fragment inserted in a reverse orientation between the XhoI and KpnI sites. Constructs expressing tagged HIB or its fragments were generated by placing the cDNA encoding for various portions of HIB between the BglII and XhoI sites of *pUAST-Flag* or *pUAST-HA* vector. To construct *UAS-Flag-Spop*, full-length SPOP cDNA was amplified by PCR from mouse E17 cDNA library (Clontech) and subcloned in the BglII and XhoI sites of the *pUAST-Flag* vector.

Generating *hib* Null Mutation by Gene Targeting
Ends-out homologous recombination was used to generate *hib* null mutation (Gong and Golic, 2003). Left and right arms of the targeting vector were prepared by PCR of ~4 kb fragments from genomic DNA

using two pairs of primers: 5′-CTCTGCGGCCGCAGAAATGCCGA
CTGCAAAG-3′/5′-GGATGCATGCAGGTTCGAGGTGACTCTAGC-3′
and 5′-AACAGGCGCGCCGTACCGTTTATTGTTTCG-3′/5′-TGTAG
GCGCGCCAACAAACACTTCAGCTTTTG-3′. Transgenic flies carry-
ing the targeting construct on the second chromosome were
crossed to flies carrying heat-inducible FLP recombinase and I-SceI
endonuclease and targeting events were mapped to the third chro-
mosome and verified by Southern blot (Gong and Golic, 2003).

Generating Clones of Marked Mutant Cells

Clones of mutant cells were generated by *FLP/FRT*-mediated mi-
totic recombination as described (Jiang and Struhl, 1995). Geno-
types for generating clones are as follows: *hib* clones in eye discs
with or without expressing UAS transgenes: *ey-flp; (GMR-Gal4/
UAS* transgenes*); FRT82 hib$^{\Delta 6}$/FRT82 hs-Myc-GFP. hib* clones in
wing discs with or without expressing UAS transgenes: *MS1096
hs-flp/(UAS-P35); (UAS-hh or UAS-HACi^{-3P}); FRT82 hib$^{\Delta 6}$/FRT82
hs-Myc-GFP. cul3* clones in wing discs expressing *UAS-Flag-HIB*:
*MS1096 hs-flp; cul3^{gft2} FRT40/hs-Myc-GFP FRT40; UAS-Flag-
HIB.9 + UAS-Flag-HIB.10/+.*

Cell Culture, Transfection, Immunoprecipitation, Western Blot, and In Vivo Ubiquitination Assay

S2 cell culture, transfection, immunoprecipitation, and immunoblot
analysis were performed with standard protocols as previously de-
scribed (Zhang et al., 2005). In vivo ubiquitination assays were based
on the protocol previously described (Wang and Li, 2006). Briefly, S2
cells were transfected in 10 cm plates with 6 μg *UAS-Myc-CiN* and
4 μg each of the following constructs: *UAS-Flag-HIB* or *UAS-Flag-
MATH* or *UAS-Flag-BTB, UAS-Flag-Cul3^{KR}* or *UAS-Flag-Cul3,
UAS-Roc1a, pMT-HA-Ub,* and *ub-Gal4.* 24 hr after transfection,
700 μM CuSO4 was added to the medium for another 24 hr to induce
HA-Ub expression. Cells were treated with 50 μM MG132 for 4 hr be-
fore harvesting. Cells were first lysed in 100 μl denaturing buffer (1%
SDS/50 mM Tris [pH 7.5], 0.5 mM EDTA/1 mM DTT). After incubation
for 5 min at 100ºC, the lysates were diluted 10× with lysis buffer and
then subjected to coimmunoprecipitation with Myc antibody, fol-
lowed by immunoblot analysis with HA antibody.

Yeast Two-Hybrid Assay and GST Fusion Protein Pull-Down Assay

Various portions of Ci were fused to the Gal4 DNA binding domain
in the *pAS2* vector, and HIB fragments were fused to the Gal4 acti-
vation domain in the *pACT2* vector. The yeast strain AH109 was
transformed with plasmids encoding the bait and prey proteins
sequentially. Protein interactions were determined according to the
standard protocol (Clontech). GST fusion proteins were produced in
E. coli, and purified with glutathione agarose beads. GST fusion pro-
tein-loaded beads were incubated with either in vitro translated
^{35}S-labled proteins or cell lysates derived from S2 cells expressing
epitope-tagged proteins at 4ºC for 1.5 hr. The beads were washed
four times with lysis buffer, followed by Western blot analysis or
autoradiogram.

Immunostaining and In Situ Hybridization

Immunostaining and in situ hybridization of imaginal discs were
done with standard protocols (Jiang and Struhl, 1995). Antibodies
used in this study: rat anti-Ci (2A) (gift form R. Holmgren), mouse
anti-Ptc (gift from I. Guerrero), rabbit anti-βGal (Cappel), mouse
anti-Flag (Sigma), mouse anti-HA (F7), mouse anti-Myc (9E10),
mouse anti-NPCP (Berkeley Antibody Company, Richmond, CA),
and rabbit anti-GFP (Santa Cruz).

Supplemental Data

Supplemental data include five figures and are available at http://
www.developmentalcell.com/cgi/content/full/10/6/719/DC1/.

References

Angers, S., Thorpe, C.J., Biechele, T.L., Goldenberg, S.J., Zheng, N.,
Maccoss, M.J., and Moon, R.T. (2006). The KLHL12-Cullin-3 ubiqui-
tin ligase negatively regulates the Wnt-beta-catenin pathway by tar-
geting Dishevelled for degradation. Nat. Cell Biol. *8*, 348–357.

Aza-Blanc, P., Lin, H.Y., Ruiz i Altaba, A., and Kornberg, T.B. (2000).
Expression of the vertebrate Gli proteins in Drosophila reveals a dis-
tribution of activator and repressor activities. Development *127*,
4293–4301.

Chen, C.H., von Kessler, D.P., Park, W., Wang, B., Ma, Y., and
Beachy, P.A. (1999). Nuclear trafficking of Cubitus interruptus in
the transcriptional regulation of Hedgehog target gene expression.
Cell *98*, 305–316.

Gong, W.J., and Golic, K.G. (2003). Ends-out, or replacement, gene
targeting in Drosophila. Proc. Natl. Acad. Sci. USA *100*, 2556–2561.

Huntzicker, E.G., Estay, I.S., Zhen, H., Lokteva, L.A., Jackson, P.K.,
and Oro, A.E. (2006). Dual degradation signals control Gli protein
stability and tumor formation. Genes Dev. *20*, 276–281.

Ingham, P.W., and McMahon, A.P. (2001). Hedgehog signaling in an-
imal development: paradigms and principles. Genes Dev. *15*, 3059–
3087.

Jia, J., and Jiang, J. (2006). Decoding the Hedgehog signal in animal
development. Cell. Mol. Life Sci., in press. Published online April 5,
2006. 10.1007/s00018-005-5519-z.

Jia, J., Amanai, K., Wang, G., Tang, J., Wang, B., and Jiang, J. (2002).
Shaggy/GSK3 antagonizes Hedgehog signaling by regulating Cubi-
tus interruptus. Nature *416*, 548–552.

Jia, J., Zhang, L., Zhang, Q., Tong, C., Wang, B., Hou, F., Amanai, K.,
and Jiang, J. (2005). Phosphorylation by double-time/CKIepsilon
and CKIalpha targets cubitus interruptus for Slimb/beta-TRCP-
mediated proteolytic processing. Dev. Cell *9*, 819–830.

Jiang, J., and Struhl, G. (1995). Protein kinase A and Hedgehog sig-
naling in *Drosophila* limb development. Cell *80*, 563–572.

Kalderon, D. (2002). Similarities between the Hedgehog and Wnt sig-
naling pathways. Trends Cell Biol. *12*, 523–531.

Kennerdell, J.R., and Carthew, R.W. (2000). Heritable gene silencing
in *Drosophila* using double-stranded RNA. Nat. Biotechnol. *18*, 896–
898.

Kent, D., Bush, E.W., and Hooper, J.E. (2006). Roadkill attenuates
Hedgehog responses through degradation of Cubitus interruptus.
Development *133*, 2001–2010.

Kwon, J.E., La, M., Oh, K.H., Oh, Y.M., Kim, G.R., Seol, J.H., Baek,
S.H., Chiba, T., Tanaka, K., Bang, O.S., et al. (2006). BTB domain-
containing speckle-type POZ protein (SPOP) serves as an adaptor
of DAXX for ubiquitination by Cul3-based ubiquitin ligase. J. Biol.
Chem. *281*, 12664–12672.

Lum, L., and Beachy, P.A. (2004). The Hedgehog response network:
sensors, switches, and routers. Science *304*, 1755–1759.

Methot, N., and Basler, K. (2000). Suppressor of Fused opposes
Hedgehog signal transduction by impeding nuclear accumulation
of the activator form of Cubitus interruptus. Development *127*,
4001–4010.

Monnier, V., Dussillol, F., Alves, G., Lamour-Isnard, C., and Plessis,
A. (1998). Suppressor of fused links fused and Cubitus interruptus on
the hedgehog signaling pathway. Curr. Biol. *8*, 583–586.

Motzny, C.K., and Holmgren, R. (1995). The *Drosophila* cubitus inter-
ruptus protein and its role in the *wingless* and *hedgehog* signal
transduction pathways. Mech. Dev. *52*, 137–150.

Ohlmeyer, J.T., and Kalderon, D. (1998). Hedgehog stimulates mat-
uration of Cubitus interruptus into a labile transcriptional activator.
Nature *396*, 749–753.

Ou, C.Y., Lin, Y.F., Chen, Y.J., and Chien, C.T. (2002). Distinct protein degradation mechanisms mediated by Cul1 and Cul3 controlling Ci stability in *Drosophila* eye development. Genes Dev. *16*, 2403–2414.

Pasca di Magliano, M., and Hebrok, M. (2003). Hedgehog signaling in cancer formation and maintenance. Nat. Rev. Cancer *3*, 903–911.

Pintard, L., Willis, J.H., Willems, A., Johnson, J.L., Srayko, M., Kurz, T., Glaser, S., Mains, P.E., Tyers, M., Bowerman, B., and Peter, M. (2003). The BTB protein MEL-26 is a substrate-specific adaptor of the CUL-3 ubiquitin-ligase. Nature *425*, 311–316.

Pintard, L., Willems, A., and Peter, M. (2004). Cullin-based ubiquitin ligases: Cul3-BTB complexes join the family. EMBO J. *23*, 1681–1687.

Price, M.A., and Kalderon, D. (2002). Proteolysis of the Hedgehog signaling effector Cubitus interruptus requires phosphorylation by Glycogen Synthase Kinase 3 and Casein Kinase 1. Cell *108*, 823–835.

Robbins, D.J., Nybakken, K.E., Kobayashi, R., Sisson, J.C., Bishop, J.M., and Therond, P.P. (1997). Hedgehog elicits signal transduction by means of a large complex containing the kinesin-related protein costal2. Cell *90*, 225–234.

Sisson, J.C., Ho, K.S., Suyama, K., and Scott, M.P. (1997). Costal2, a novel kinesin-related protein in the Hedgehog signaling pathway. Cell *90*, 235–245.

Smelkinson, M.G., and Kalderon, D. (2006). Processing of the *Drosophila* hedgehog signaling effector Ci-155 to the repressor Ci-75 is mediated by direct binding to the SCF component slimb. Curr. Biol. *16*, 110–116.

Stamataki, D., Ulloa, F., Tsoni, S.V., Mynett, A., and Briscoe, J. (2005). A gradient of Gli activity mediates graded Sonic Hedgehog signaling in the neural tube. Genes Dev. *19*, 626–641.

Stogios, P.J., Downs, G.S., Jauhal, J.J., Nandra, S.K., and Prive, G.G. (2005). Sequence and structural analysis of BTB domain proteins. Genome Biol. *6*, R82.

Treisman, J.E., and Heberlein, U. (1998). Eye development in *Drosophila*: formation of the eye field and control of differentiation. Curr. Top. Dev. Biol. *39*, 119–158.

Villavicencio, E.H., Walterhouse, D.O., and Iannaccone, P.M. (2000). The sonic hedgehog-patched-gli pathway in human development and disease. Am. J. Hum. Genet. *67*, 1047–1054.

Wang, B., and Li, Y. (2006). Evidence for the direct involvement of {beta}TrCP in Gli3 protein processing. Proc. Natl. Acad. Sci. USA *103*, 33–38.

Wang, G., Wang, B., and Jiang, J. (1999). Protein kinase A antagonizes Hedgehog signaling by regulating both the activator and repressor forms of Cubitus interruptus. Genes Dev. *13*, 2828–2837.

Wang, G., Amanai, K., Wang, B., and Jiang, J. (2000). Interactions with Costal2 and suppressor of fused regulate nuclear translocation and activity of cubitus interruptus. Genes Dev. *14*, 2893–2905.

Wu, J.T., Lin, H.C., Hu, Y.C., and Chien, C.T. (2005). Neddylation and deneddylation regulate Cul1 and Cul3 protein accumulation. Nat. Cell Biol. *7*, 1014–1020.

Xu, L., Wei, Y., Reboul, J., Vaglio, P., Shin, T.H., Vidal, M., Elledge, S.J., and Harper, J.W. (2003). BTB proteins are substrate-specific adaptors in an SCF-like modular ubiquitin ligase containing CUL-3. Nature *425*, 316–321.

Zhang, W., Zhao, Y., Tong, C., Wang, G., Wang, B., Jia, J., and Jiang, J. (2005). Hedgehog-regulated costal2-kinase complexes control phosphorylation and proteolytic processing of cubitus interruptus. Dev. Cell *8*, 267–278.